

Spatially encoded localized wavepackets for ultrafast optical data transfer

R. Grunwald
grunwald@mbi-berlin.de

Max Born Institute for Nonlinear Optics and Short-Pulse Spectroscopy Max-Born-Strasse 2a, 12489 Berlin, Germany

M. Bock

Max Born Institute for Nonlinear Optics and Short-Pulse Spectroscopy Max-Born-Strasse 2a, 12489 Berlin, Germany

Arrays of highly localized wavepackets enable for an efficient multichannel processing of optical data because of their undistorted propagation in space and time domain. Reconfigurable arrangements of supercollimated and temporally nondiffracting few-cycle pulses were generated by microaxicons programmed into the phase map of a liquid-crystal-on-silicon spatial light modulator. As an example, the transfer of quick response code data with few-femtosecond pulses of a Ti:sapphire laser oscillator is reported. Data encoding in beam arrays via maps of temporal and spectral moments is proposed. [DOI: <http://dx.doi.org/10.2971/jeos.2012.12009>]

Keywords: Ultrashort pulses, localized wavepackets, optical communication, nondiffracting beams, encoding

1 INTRODUCTION

The high achievable spatial and temporal localization of photons in quasi-nondiffracting (QND) ultrashort-pulsed wavepackets [1] enables for transporting energy as well as information over larger distances with slower decay and higher stability compared to pulsed polychromatic Gaussian beams. The combination of the advantageous properties of QND pulses with addressable multichannel architectures with individually programmable sub-beams stimulates applications like adaptive measuring techniques, advanced pulse diagnostic systems, space-variant plasmon excitation, flexible nanomachining or optical communication and computing. In particular, recently demonstrated two-dimensional binary "flying images" [2] composed of QND-sub-beams promise a more robust, high-speed transfer of structured light fields with low cross-talk over extended propagation paths.

In first experimental implementations, variable microaxicon phase functions were programmed into the gray value map of a high-resolution liquid-crystal-on-silicon spatial light modulator (LCoS-SLM) generating an addressable matrix of particular QND beams. These beams which we refer to as "needle beams" [1], [3]–[5] represent the central lobes of Bessel beams and, similar to the case of Gaussian beams, do not contain outer fringes. Therefore, the intensity profile of a needle beam is described by the square of a Bessel function within the limits of the first zeros. Like Bessel beams, needle beams show extended focal zones, a high angular tolerance [6, 7] and behave self-reconstructing [1]. Another unique property of ultrashort-pulsed needle beams consists in their capability to propagate with a quasi-nondiffracting characteristics in spatial as well as temporal domain over significantly extended range as it was clearly indicated in experiments with few-cycle pulses [8]. All the mentioned features make

the concept of programmable needle beam arrays particularly attractive for ultrafast data transfer, processing and storage in planar-optical as well as free-space communication systems.

Here we report on recent studies of ultrafast information transfer with complex QND patterns composed of microscopic needle beams and related types of highly localized wavepackets (HLWs) [9]. As an application example, the ultrafast transfer of binary quick response (QR) data with few-cycle pulsed needle beams is demonstrated for the first time. Further approaches to encode image information in spatial maps of spectral and temporal pulse parameters of programmable needle beam arrays are proposed.

2 Experimental Techniques

A few-cycle Ti:sapphire laser oscillator (VENTEON PULSE: ONE PE, center wavelength 800 nm, minimum pulse duration 6 fs, FWHM spectral bandwidth 300 nm, pulse energy 7 nJ, repetition frequency 80 MHz) was used as the light source. For input pulse durations below 10 fs, the dispersion of the optical components was pre-compensated by a pair of chirped mirrors. Complex patterns were programmed into the phase maps of reflective, phase-only LCoS-SLMs. The SLMs were calibrated with respect to their gray-level dependent spectral phase response. It was found that minimum residual phase distortions were caused by Gires-Tournois interference [10]. Figure 1 shows the setup for generating and detecting programmable flying images. Two-dimensional binary image information was translated into a reconfigurable arrangement of axicons (bit) and voids (no bit). The axicons transfer the amplitude information into a corresponding

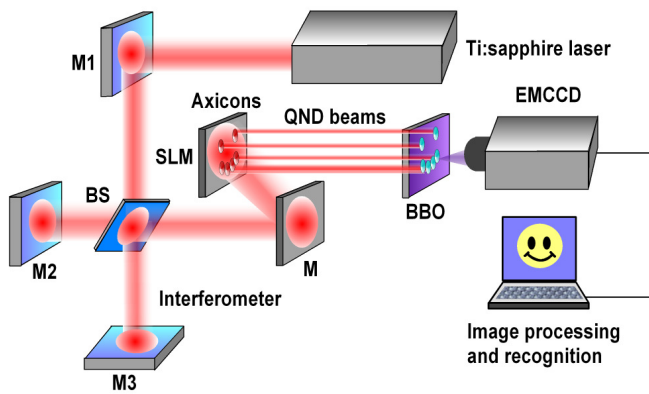


FIG. 1 Experimental setup for the generation of spatially and temporally encoded quasi-nondiffracting (QND) patterns (schematically). Image information is encoded in the phase map of a reflective spatial light modulator (SLM) by programming a reconfigurable arrangement of axicons (M = beam redirecting mirror). The axicons generate pulsed needle beams the intensity patterns of which are detected by a sensitive EMCCD camera (drawn) or other types of CCD cameras. For the recognition of temporal maps, two-dimensional second-order autocorrelation is implemented by including a Michelson interferometer (mirrors M_1 , M_2 , M_3 and a BBO crystal for frequency conversion via second harmonic generation). Intensity patterns and 2D autocorrelation data are analysed with adapted image processing software.

arrangement of ultrashort-pulsed QND sub-beams. For the detection of time-integrated intensity patterns we used either CCD or EMCCD matrix cameras depending on the necessary sensitivity. Pulse duration maps were determined by collinear second order autocorrelation [11]. Because of working with an array of separated (cross-talk-free) pulsed needle beams, a simultaneous multichannel autocorrelation independently on the envelope wavefront curvature is enabled. The resulting spatial resolution is given by the period of the programmed array of axicons. The distinct tilt tolerance of axicons [6, 7] facilitates the off-axis illumination of the reflective SLMs up to relatively large incident angles. Anamorphic image distortions can also be corrected adaptively [12].

3 Nondiffracting transfer of a QR-code

In this first experiment, a matrix consisting of $29 \times 29 = 841$ conical elements (microaxicons) was used to shape flexible ultrashort-pulsed flying images for free-space optical data transfer. With graphics software, phase patterns were written in an LCR 1080 SLM (HoloEye; maximum phase step 1π at 800 nm, 2 million pixels, pixel size $8.1 \times 8.1 \mu\text{m}^2$). Geometry and arrangement of the axicons (conical angle, period, shape and symmetry) were individually programmable. A two-dimensional quick response (QR-) code (corresponding to the internet link of the MBI homepage) was programmed with a barcode generator freeware (Byte Scout) and translated to a binary amplitude map of the SLM. The conditions for a stable readout were carefully studied for a given detection system with respect to the tolerable fill factor and noise level. It was found that the linear fill factor (concerning to the connecting line between two neighbouring spots) has to be larger than $F = 0.5$ and the tolerable added noise signal was about 90%

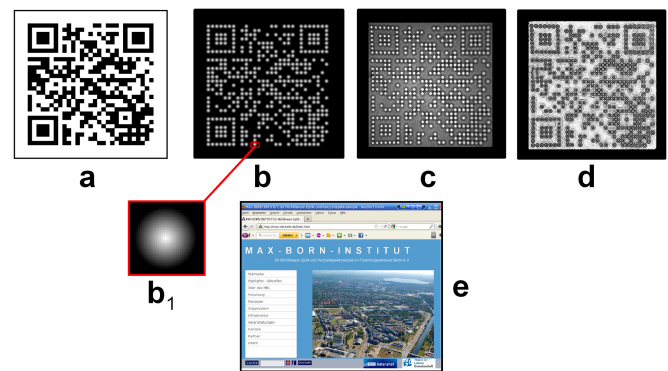


FIG. 2 Ultrafast image transfer with arrays of micro-scale quasi-nondiffracting wavepackets possessing supercollimation (needle beams) and high temporal stability, (a) QR encoded amplitude pattern, (b) corresponding 29×29 gray value matrix, (b₁) gray value distribution of an individual element of this matrix, (c) corresponding needle beam array generated with an LCoS-SLM, (d) post-processed image, (e) decoded link (MBI homepage); laser: Ti:sapphire oscillator (center wavelength 800 nm, pulse duration 6 fs).

of the standard deviation of the signal. Figure 2 shows (a) an ideal binary pattern, (b) the corresponding phase map written in the SLM, (c) the realized matrix of sub-beams after an axial propagation distance of $z = 4$ mm (12 pixels per axicon, axicon diameter about $100 \mu\text{m}$, vertex phase: 1π), and (e) the detected pattern (here, the detector was an iPhone 4 camera with 5 million pixels) after post-processing with an appropriate image processing software. The pattern was flipped horizontally, the amplitude was inverted, and the relevant spatial frequencies were filtered out. The distance-to-diameter ratio at the used measuring distance was 40:1. It was found to be important to eliminate any dark rim structures in this procedure. To recognize the pattern, an available QR scanning code (QR Code City) was applied. In further experiments, we demonstrated the QND characteristics of complex-shaped wavepackets also consisting of non-circular components like lines and elliptical compartments which still remain their supercollimation properties and temporal pulse information (i.e. a stable pulse duration within a tolerance of about 1 fs).

4 Temporal and spectral maps

As it was shown above, the LCoS-technique enables to realize refractive components of variable shape or focal length by encoding different phase levels via discrete gray-values (taking into account corresponding calibration curves). Apart from refractive beam steering, however, it can be applied to encode arrays of pulses in time domain and spectral domain. This can be done in different ways:

(i) The minimum phase step defines the resolution of the optical path which is directly coupled to the travelling time of the pulses. Thus, maps of slightly modified arrival times of an array of QND sub-beams can be generated and detected by nonlinear multichannel autocorrelation. The relative measurement is self-referential. Figure 3(a) and 3(b) show the principle of time delay encoding for a linear array of

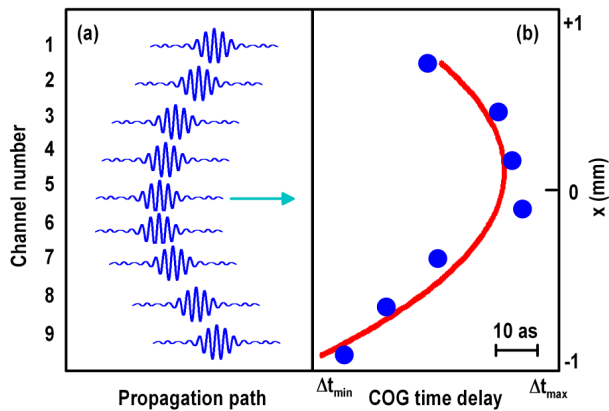


FIG. 3 Principle of temporal mapping: (a) channel dependent travel time of ultra-short wavepackets corresponding to individual QND sub-beams (spatial snapshot with offsets, schematically; arrow: propagation direction); (b) measured relative temporal delay profile $\Delta t(x)$ of the centers of gravity (COG) of individual wavepackets after passing a lens-like phase function (initial pulse duration: 6 fs, spatial period: 350 μm). The autocorrelation was performed with sub-femtosecond time resolution (step width of interferometer arm: 20 nm, time integration over 0.6×10^7 pulses, spatially averaged over each individual needle beam).

QND sub-beams and the spatial distribution function of the temporal delay of a 6-fs pulse after shaping with a radially variable phase derived from a multichannel second order autocorrelation measurement, respectively.

(ii) Statistical temporal moments describing the length and the shape of the individual pulses can be modified and analysed with the autocorrelation. In both cases, a spatial pattern can be retrieved from temporal autocorrelation data if the temporal resolution of the detection system and/or the phase stability allow to separate the signal from noise. Improvements can be obtained by a carrier envelope offset (CEO) stabilization.

(iii) Spectral statistical moments can be written in a similar way. For transform-limited (chirp-free) pulses, the maps of temporal and spectral moments can directly be converted to each other by Fourier transform. In the presence of chirp effects, the relationship is more complicated. In all cases, the contrast must be sufficiently high for a reliable reconstruction of relevant image features.

5 Conclusions

To conclude, the flexible generation of structured non-diffracting few-cycle wavepackets with an LCoS-SLM was performed. QR code data transfer with high-element-number flying images consisting of up to 841 quasi-nondiffracting needle beams was demonstrated. It was shown that non-circular sub-beams can be used to compose even more complex patterns without losing supercollimation, re-

business and temporal properties. The technique promises further applications to spatially selective excitation of plasmons, wavefront sensing and measuring techniques. Further methods to encode image information in ultrashort pulses based on temporal and spectral maps in combination with a two-dimensional nonlinear autocorrelator as detection system are proposed.

Acknowledgements

The authors thank T. Elsaesser (MBI), S. Osten (HoloEye GmbH, Berlin), J. Jahns (FernUniversity, Hagen), P. Saari (University Tartu), A. Friberg (University Helsinki), M. Piché (Laval University, Quebec) and C. Fischer (metrolux GmbH, Gttingen) for support and discussions. The work was granted by DFG under contract GR1782/13-1.

References

- [1] M. Zamboni-Rached, E. Recami, H. E. Hernández-Figueroa, eds., *Localized Waves, Theory and experiments* (Wiley & Sons, New York, 2008).
- [2] P. Saari, "Spatially and temporally nondiffracting ultrashort pulses," in *Ultrafast Processing Spectroscopy*, O. Svelto, S. De Silvestri, and G. Denardo, eds., 151-156 (Plenum Press, New York, 1996).
- [3] R. Grunwald, *Thin-film microoptics - new frontiers of spatio-temporal beam shaping* (Elsevier, Amsterdam, 2007).
- [4] R. Grunwald, and M. Bock, "Programmable microoptics for ultrashort pulses," *SPIE Proc. Ser.* **7716**, 77160P (2010).
- [5] R. Grunwald, M. Bock, V. Keibel, S. Huferath, U. Neumann, G. Steinmeyer, G. Stibenz, J.-L. Néron, and M. Piché, "Ultrashort-pulsed truncated polychromatic Bessel-Gauss beams," *Opt. Express* **16**, 1077-1089 (2008).
- [6] R. Grunwald, S. Huferath, M. Bock, U. Neumann, and S. Langer, "Angular tolerance of Shack-Hartmann wavefront sensors with microaxicons," *Opt. Lett.* **32**, 1533-1535 (2007).
- [7] T. Tanaka, and S. Yamamoto, "Comparison of aberration between axicon and lens," *Opt. Commun.* **184**, 113-118 (2000).
- [8] M. Bock, S. K. Das, and R. Grunwald, "Programmable ultrashort-pulsed flying images," *Opt. Express* **17**, 7465-7478 (2009).
- [9] M. Bock, S. K. Das, and R. Grunwald, "Adaptive shaping of complex pulsed nondiffracting light fields," *SPIE Proc. Ser.* **7950**, 7950-8 (2011).
- [10] M. Bock, S. K. Das, R. Grunwald, S. Osten, P. Staudt, and G. Stibenz, "Spectral and temporal response of liquid-crystal-on-silicon spatial light modulators," *Appl. Phys. Lett.* **92**, 151105 (2008).
- [11] M. R. Grunwald, U. Neumann, U. Griebner, K. Reimann, G. Steinmeyer, V. Keibel, "Ultrashort-pulse wavefront autocorrelation," *Opt. Lett.* **28**, 2399-2401 (2003).
- [12] M. Bock, S. K. Das, C. Fischer, M. Diehl, P. Börner, and R. Grunwald, "Reconfigurable wavefront sensor for ultrashort pulses," *Opt. Lett.* **37**, 1154-1156 (2012).